Ultra-wideband Transmitted Reference Systems

Yi-Ling Chao and Robert A. Scholtz, *Life Fellow, IEEE*

***Abstract*— This paper derives optimal receiver structures for an ultra-wideband transmitted reference (UWB TR) system in multipath environments, based on the average likelihood ratio test (ALRT) with Rayleigh or lognormal path strength models. Several suboptimal receivers are obtained by either applying an approximation to the log-likelihood function without any specific channel statistical models or by approximating two ALRT optimal receiver structures. It is shown that the generalized likelihood ratio test optimal receiver [9] is one of the suboptimal receiver structures in the ALRT sense. Average bit error probabilities of ALRT receivers are evaluated. Results show that ALRT optimal and suboptimal receivers derived from Rayleigh and lognormal models can perform equally well in each other's environments. This paper also investigates *ad hoc* cross-correlation receivers in detail, and discusses the equivalence between cross-correlation receivers and one theoretically derived ALRT suboptimal receiver. Results show that the noise $\times$ noise term in a cross-correlation receiver can be modelled quite accurately by a Gaussian random variable when the noise time$\times$bandwidth product is large, and cross-correlation receivers are suboptimal structures which have worse performance than ALRT receivers.**

***Index Terms*— Ultra-wideband radio, transmitted reference system, multipath environments, average likelihood ratio test, generalized likelihood ratio test, *ad hoc* cross-correlation receiver.**

I. Introduction

Ultra-wideband (UWB) impulse radio systems, because of their fine time-resolution capability, could make use of Rake receivers with tens or even hundreds of correlation operations to take full advantage of the available signal energy in an indoor environment [2], [3]. Instead of using Rake reception, Hoctor and Tomlinson proposed a UWB transmitted reference (TR) system with a simple receiver structure to capture all the energy available in a UWB multipath channel [7]. The transmitted reference technique dates back to the early days of communication theory when it was explored as a means for establishing communication when there are critical unknown properties of the transmitted signal or channel [4], [5], [6].

In a TR modulation format (described in detail in Section II), a reference pulse is transmitted before each data-modulated pulse for the purpose of determining the current multipath channel response. The conventional TR cross-correlation receiver correlates the received data signal with the received reference signal to use all the energy of the data signal without requiring additional channel estimation and Rake reception. This suboptimal receiver is easy to implement, requiring only an analog delay line to align the received reference and data pulses. The analog-to-digital converter (ADC), which samples and quantizes the correlator's output, is less susceptible to timing noise, and operates at a frequency much lower than that required by a fully digital receiver.

Yi-Ling Chao (yilingch@usc.edu) was a graduate student and Robert Scholtz (scholtz@usc.edu) is a Professor with the Department of Electrical Engineering at the University of Southern California. This work was supported by the Army Research Office under MURI Grant No. DAAD19-01-1-0477.

The conventional cross-correlation receiver is restricted by two major drawbacks: (1) the transmitted reference signal used as a correlator template is noisy, and (2) a fraction of the transmitted energy is not data bearing. Average multiple reference pulses to produce a cleaner template can improve the receiver performance [8], [9], but these cross-correlation receivers are *ad hoc* receivers, and how well a more general UWB TR system can perform is still a complicated function of channel descriptions/statistics and channel stability, as well as complexity constraints on the receiver. When complexity constraints are removed or relaxed, more exotic channel estimation techniques and Rake receivers are design possibilities that provide better performance (at a higher complexity cost) than *ad hoc* TR receivers, and in this case the utility of devoting energy to the reference signal is questionable.

This paper derives optimal (see Section III) and related suboptimal (see Section IV) receiver structures using either the average likelihood ratio test (ALRT) with Rayleigh or lognormal path strength models, along with a suboptimal receiver without any specific statistical models for the path strength. In these analyses, a simplifying resolvable multipath assumption is employed which is valid in channel environments in which the time difference between every two multipath signal components is greater than a direct-path pulse width. When the transmitted pulse width in a UWB system is less than a nanosecond, this resolvable multipath assumption applies when differential propagation path lengths are always greater than one foot. In reality, because of its short duration, a pulse received over a single propagation path may only overlap in time and correlate with few other multipath component pulses. Therefore, even if the resolvable multipath assumption is not exactly true in some environments, it may still provide a reasonable approximation to real channel models.

The nonlinear operation of these optimal and suboptimal receivers makes theoretical bit-error probability (BEP) analyses difficult, and numerical simulations are employed with two ALRT suboptimal receivers as the only exception. In addition, we also investigate *ad hoc* cross-correlation receivers further, discuss the equivalence between the cross-correlation receivers and one theoretically derived ALRT suboptimal receiver, and validate the Gaussian approximation to the distribution of the noise$\times$noise term when the noise time$\times$bandwidth product is large enough in Section V. Section VI evaluates the average BEP of optimal and suboptimal receivers numerically. Conclusions are given in Section VII.

II. UWB TR Modulation and Received Signals

The transmitted signal of a UWB TR system with antipodal modulation is

$$s_{\text{tr}}(t) = \sum_{i=-\infty}^{\infty} g_{\text{tr}}(t - iT_{\text{f}}) + b_{\lfloor i/N_{\text{s}} \rfloor} g_{\text{tr}}(t - iT_{\text{f}} - T_{\text{d}}). \quad (1)$$

Here $g_{\text{tr}}(t)$ is a transmitted monocycle waveform that is non-zero only for $t \in (0, T_{\text{w}})$, and T_{f} is the frame time. Each frame contains two monocycle waveforms. The first is a reference and the second, T_{d} seconds later, is a data-modulated waveform. For analytical purposes, the data bit stream is assumed to be composed of independent, identically distributed binary random variables $b_{\lfloor i/N_{\text{s}} \rfloor} \in \{1, -1\}$, taking on either value with probability $1/2$. The index $\lfloor i/N_{\text{s}} \rfloor$, i.e., the integer part of i/N_{s}, represents the index of the data bit modulating the data waveform in the i^{th} frame. Hence each bit is transmitted in N_{s} successive frames to achieve an adequate bit energy in the receiver, and the channel is assumed invariant over one bit time.

In this TR system, T_{d} is greater than or equal to the multipath delay spread T_{mds} to assure that there is no interference between reference signal and data signal. The frame time T_{f} is chosen to satisfy $T_{\text{f}} \geq 2T_{\text{d}} \geq 2T_{\text{mds}}$ so that no interframe interference exists. The discussion of inter-pulse-interference in a UWB TR system can be found in [22] and [23]. For simplicity but without loss of generality, the time-hopping or direct sequence modulation which is used to reduce multiuser interference is not modelled because only the single user case is considered here. A simplified example of the transmitted and received signals for bits $b_0 = -1$ and $b_1 = 1$ are shown in Figure 1 to illustrate TR timing and modulation structure. In this figure, the letter R represents the reference pulse, the letter D represents the data pulse, and $T_{\text{d}} = T_{\text{mds}}$.

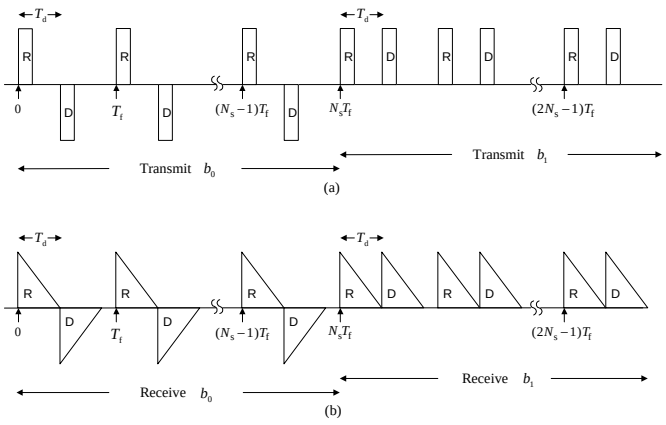

Fig. 1. An example of (a) transmitted signal and (b) received signal with $b_0 = -1$ and $b_1 = 1$.

The received TR signal of bit b_0 is modelled as

$$r(t) = r_{\text{s}}(t) + n(u, t), \quad (2)$$

where $n(u, t)$ represents Gaussian receiver noise with two-sided power spectral density $\frac{N_0}{2}$, and

$$r_{\text{s}}(t) = \sum_{i=0}^{N_{\text{s}}-1} [g(t - iT_{\text{f}}) + b_0 g(t - iT_{\text{f}} - T_{\text{d}})], \quad (3)$$

where a received waveform $g(t)$ is modelled as the output of a tapped delay line channel

$$g(t) = \sum_{k=0}^{K-1} p_k \alpha_k g_{\text{rx}}(t - k\Delta), \quad (4)$$

Δ being the width of a resolvable time slot and $K\Delta$ being the channel delay spread. We also assume that $p_k \alpha_k$ in different time slots k are independent. The polarity p_k of the multipath signal component in time slot k is in $\{+1, -1\}$ with equal probability so the probability density function is

$$f(p_k) = \frac{1}{2}\delta_{\text{D}}(p_k - 1) + \frac{1}{2}\delta_{\text{D}}(p_k + 1), \quad (5)$$

and the amplitude α_k, which is independent of p_k, has mixture distribution such that α_k is equal to zero with probability $1 - a$ and is occupied with an arrival with probability a

$$f(\alpha_k) = a \times f(\alpha_k | \text{slot } k \text{ occupied}) + (1 - a)\delta_{\text{D}}(\alpha_k), \quad (6)$$

where $f(\alpha_k | \text{slot } k \text{ occupied})$ can be a Rayleigh or lognormal distribution in this paper.

The received monocycle waveform $g_{\text{rx}}(t)$ of a single multipath component, normalized to unit energy, i.e., $\int_{-\infty}^{\infty} g_{\text{rx}}^2(t)dt = 1$, will differ in shape from the transmitted waveform, and its shape may vary for different multipath components [11], [12]. In the design and analysis of ALRT receivers, we assume that $g_{\text{rx}}(t)$ is known and is the same for all multipath components, and can be used as a template in a correlator. The average energy in the k^{th} path component is

$$2N_{\text{s}}\mathbb{E}\{\alpha_k^2\} = 2N_{\text{s}}a\mathbb{E}\{\alpha_k^2 | \text{slot } k \text{ occupied}\}$$

due to the normalization of $g_{\text{rx}}(t)$, and the average path signal-energy-to-noise-power-density-ratio (ASNR) as well as the realized path signal-energy-to-noise-power-density-ratio (RSNR) in the k^{th} path component are defined as $\text{ASNR}_k = \frac{2N_{\text{s}}\mathbb{E}\{\alpha_k^2\}}{N_0}$ and $\text{RSNR}_k = \frac{2N_{\text{s}}\alpha_k^2}{N_0}$.

III. ALRT Optimal Receivers

We now detect the bit b_0 based on the observation $\tilde{r}$ of $r(t)$, $t \in (0, N_{\text{s}}T_{\text{f}})$. Using the ALRT which minimizes the average bit error probability, the decision rule is of the form

$$\frac{p(\tilde{r}|b_0 = 1)}{p(\tilde{r}|b_0 = -1)} \underset{-1}{\overset{1}{\gtrless}} 1. \quad (7)$$

Defining $\boldsymbol{\alpha} \triangleq [\alpha_0, \alpha_1, ..., \alpha_{K-1}]$ and $\boldsymbol{p} \triangleq [p_0, p_1, ..., p_{K-1}]$, $p(\tilde{r}|b_0 = 1)$ and $p(\tilde{r}|b_0 = -1)$ are averages of

$$p(\tilde{r}|b_0 = \pm 1, \boldsymbol{p}, \boldsymbol{\alpha}) \equiv \exp\left\{-\frac{1}{N_0}\int_0^{N_{\text{s}}T_{\text{f}}} [r(t) - r_{\text{s}}(t)]^2 dt\right\} \quad (8)$$

over $\boldsymbol{\alpha}$ and $\boldsymbol{p}$ which along with b_0 are imbedded in $r_{\text{s}}(t)$, and equivalence ($\equiv$) indicates that irrelevant constants have been dropped. By using the assumptions that $\boldsymbol{\alpha}$ and $\boldsymbol{p}$ are independent as well as that resolvable multipath signal components

are statistically independent, the probability density function, $f(\boldsymbol{\alpha}, \boldsymbol{p})$ can be decomposed as

$$f(\boldsymbol{\alpha}, \boldsymbol{p}) = \prod_{k=0}^{K-1} f(\alpha_k) f(p_k).$$

By applying the resolvable multipath assumption to eliminate the cross-correlation of any two pulses in (8) in the averaging process, and taking natural logarithm in both sides of (7), the ALRT rule can be reduced to

$$\sum_{k=0}^{K-1} L_k(C(k)) \underset{-1}{\overset{1}{\gtrless}} \sum_{k=0}^{K-1} L_k(D(k)), \tag{9}$$

in which the log-likelihood function $L_k(x)$ is defined as

$$L_k(x) = \ln \left[\int_{-\infty}^{\infty} \int_{-\infty}^{\infty} f(\alpha_k) f(p_k) \times \exp\left(p_k \alpha_k x - \frac{2N_\mathrm{s}}{N_0} \alpha_k^2 \right) d\alpha_k dp_k \right], \tag{10}$$

and the quantities $C(k)$ and $D(k)$ are

$$C(k) \triangleq \frac{2}{N_0}[C_\mathrm{R}(k) + C_\mathrm{D}(k)],$$
$$D(k) \triangleq \frac{2}{N_0}[C_\mathrm{R}(k) - C_\mathrm{D}(k)],$$

where

$$C_\mathrm{R}(k) \triangleq \sum_{i=0}^{N_\mathrm{s}-1} \int_0^{N_\mathrm{s}T_\mathrm{f}} r(t) g_\mathrm{rx}(t - iT_\mathrm{f} - k\Delta) dt,$$
$$C_\mathrm{D}(k) \triangleq \sum_{i=0}^{N_\mathrm{s}-1} \int_0^{N_\mathrm{s}T_\mathrm{f}} r(t) g_\mathrm{rx}(t - iT_\mathrm{f} - T_\mathrm{d} - k\Delta) dt.$$

In (9), the received signal information is embedded in $C(k)$ and $D(k)$ for $k = 0, 1, \ldots, K-1$. The optimal receiver structure always has signal processors with $C(k)$ and $D(k)$ as inputs no matter what the distributions of $\boldsymbol{p}$ and $\boldsymbol{\alpha}$ are, and is shown in Figure 2.

A. Rayleigh Path Strength Models

The Rayleigh distribution is often used in modelling signal amplitudes in wireless channels, and the probability density function of the amplitude α_k of an arrival is

$$f\left(\alpha_k | \text{ slot } k \text{ occupied}\right) = \frac{\alpha_k}{\sigma_k^2} \exp\left\{ -\frac{\alpha_k^2}{2\sigma_k^2} \right\} \quad \alpha_k > 0, \tag{11}$$

where $2\sigma_k^2 = \mathbb{E}\{\alpha_k^2 | \text{slot } k \text{ occupied}\}$. Using (5), (6) and (11), the log-likelihood function in (10) in the Rayleigh case is computed in Appendix II. This computation contains the positive parameter

$$w_\mathrm{R}(k) \triangleq \frac{\sigma_k^2}{1 + SNR_k},$$

where $SNR_k = \frac{4N_\mathrm{s}\sigma_k^2}{N_0}$ is twice the ratio of the average energy in the occupied k^{th} time slot to the noise power density. By eliminating those terms in (48) which are same for both the $b_0 = 1$ and $b_0 = -1$ cases and have no effect on the decision, the log-likelihood function becomes

$$L_k(x) = \frac{w_\mathrm{R}(k)x^2}{2} + \ln\left\{ \exp\left(-\frac{w_\mathrm{R}(k)x^2}{2} \right) + \sqrt{\frac{\pi w_\mathrm{R}(k)x^2}{2}} \left(1 - 2Q\left(\sqrt{w_\mathrm{R}(k)x^2} \right) \right) + \left(\frac{1-a}{a} \right) (1 + SNR_k) \exp\left(-\frac{w_\mathrm{R}(k)x^2}{2} \right) \right\}. \tag{12}$$

(ALRT Rayleigh receiver)

This function is monotone increasing in x.

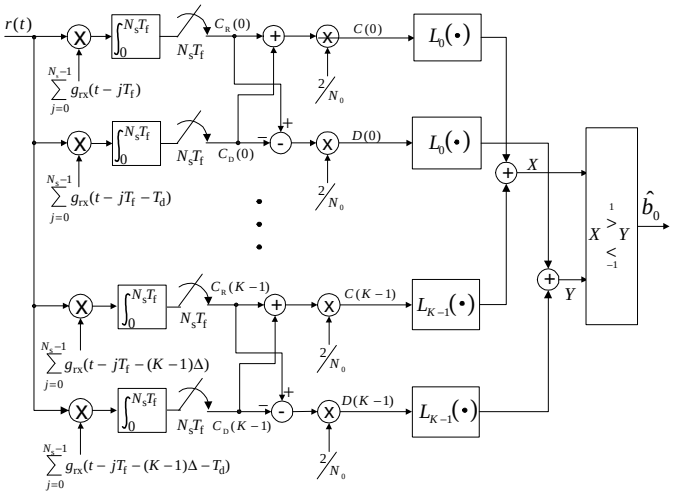

Fig. 2. The block diagram of the ALRT optimal receiver in which $X = \sum_{k=0}^{K-1} L_k(C(k))$ and $Y = \sum_{k=0}^{K-1} L_k(D(k))$.

B. Lognormal Path Strength Models

The lognormal distribution is used in the UWB channel model proposed by the IEEE 802.15.3a working group [10], and the probability density function of the amplitude α_k of an arrival is

$$f(\alpha_k | \text{slot } k \text{ occupied}) = \frac{20}{\ln 10 \sqrt{2\pi\sigma^2}\alpha_k} \times \exp\left\{ -\frac{(20\log\alpha_k - \mu_k)^2}{2\sigma^2} \right\} \quad \alpha_k > 0, \tag{13}$$

i.e., $20\log\alpha_k \sim \text{Normal}(\mu_k, \sigma^2)$. The function $\log(\cdot)$ is a 10-based logarithm, μ_k (decibels) and σ (decibels) are the mean and standard deviation of $20\log\alpha_k$, respectively. In order to make a decision on b_0, we use (6), (13), and (10), as well as change variables by letting $y_k = 20\log\alpha_k$ and $\beta_k = \frac{y_k - \mu_k}{\sqrt{2\sigma^2}}$. The nuisance parameter α_k can be eliminated to give

$$L_k(x) = \ln\left\{ \int_{-\infty}^{\infty} f(p_k) \left[(1-a) + a \int_{-\infty}^{\infty} \exp(-\beta_k^2) \times \exp\left(x p_k 10^{\frac{\sqrt{2}\sigma\beta_k + \mu_k}{20}} - \frac{2N_\mathrm{s}}{N_0} \cdot 10^{\frac{2(\sqrt{2}\sigma\beta_k + \mu_k)}{20}} \right) d\beta_k \right] dp_k \right\}. \tag{14}$$

There is no closed-form simplification when a lognormal distribution is involved in an integral. But we can use the Hermite-Gauss integral [18] to simplify the inner integral in

(14). The Hermite-Gauss integral is (see [14], equation 25.4.46 and Table 25.10)

$$\int_{-\infty}^{\infty} e^{-x^2} f(x)dx = \sum_{i=1}^{N} \omega_i f(x_i) + R_N, \qquad (15)$$

where x_i is the i^{th} zero of $H_N(x)$, a Hermite polynomial. The weights ω_i and remainder R_N are defined as

$$\begin{aligned} \omega_i &\triangleq \frac{2^{n-1}N!\sqrt{\pi}}{N^2[H_{N-1}(x_i)]^2}, \\ R_N &\triangleq \frac{N!\sqrt{\pi}}{2^n(2N)!} f^{(2N)}(\xi), \qquad -\infty < \xi < \infty. \end{aligned}$$

The smaller the absolute value of x_i is, the larger the corresponding weight w_i is. Usually R_N becomes very small when $N \geq 20$, and can be ignored.

By applying (5), (15), and the definitions

$$w_{\text{L}}(k) \triangleq 10^{\frac{\mu_k}{20}}, \qquad h(i) \triangleq 10^{\frac{\sqrt{2}\sigma x_i}{20}},$$

(14) is further simplified to

$$\begin{aligned} L_k(x) = \ln \Bigg\{ & a \sum_{i=1}^{N} \omega_i \exp\left[-\frac{2N_{\text{s}}}{N_0} h^2(i) w_{\text{L}}^2(k)\right] \\ & \times \cosh[h(i) w_{\text{L}}(k) x] + 1 - a \Bigg\}, \end{aligned} \qquad (16)$$

(ALRT lognormal receiver with N)

in which the remainder R_N is discarded. This function is monotone increasing in x. The effect of eliminating R_N on the BEP performance is tested for different values of N in Section VI by simulation.

IV. ALRT Suboptimal Receivers

In the beginning of this section, a delta function approximation is applied in a general sense without any specific statistical models of path amplitudes to obtain a suboptimal receiver structure. The suboptimal receivers, which approximate the ALRT optimal receivers with Rayleigh and lognormal path strength models, will be derived in next two subsections.

Suboptimal receivers use simple structures to approximate the log-likelihood function $L_k(\cdot)$ in (10). The integration over p_k can be carried out first to result in

$$\begin{aligned} L_k(x) &= \ln \Bigg\{ \frac{1}{2} \int_0^{\infty} f(\alpha_k) \left[\exp\left(\alpha_k x - \frac{2N_{\text{s}}}{N_0} \alpha_k^2 \right) \right. \\ &\qquad \left. + \exp\left(-\alpha_k x - \frac{2N_{\text{s}}}{N_0} \alpha_k^2 \right) \right] d\alpha_k \Bigg\} \\ &= \ln \Bigg\{ \frac{k'(x)}{2} \int_0^{\infty} f(\varrho_k) \left[N_{\varrho_k}(m'_+(x), {\rho'_k}^2) \right. \\ &\qquad \left. + N_{\varrho_k}(m'_-(x), {\rho'_k}^2) \right] d\varrho_k \Bigg\} \end{aligned} \qquad (17)$$

where $\alpha_k = \rho_k \varrho_k$ with ϱ_k being a unit second moment random variable and ρ_k^2 being the possibly unknown second moment of α_k, $f(\varrho_k)$ is the density function of ϱ_k which might include a dirac delta function in it and can be written as $f(\varrho_k) = f'(\varrho_k) + \varpi \delta_{\text{D}}(\varrho_k - \psi)$ with $0 \leq \varpi \leq 1$, $N_{\varrho_k}(\cdot)$ represents a normal density function in the variable ϱ_k with mean $m'_+(x)$ or $m'_-(x)$ and variance ${\rho'_k}^2$, and

$$\begin{aligned} k'(x) &= \sqrt{\frac{\pi N_0}{2N_{\text{s}}\rho_k^2}} \exp\left\{ \frac{x^2 N_0}{8N_{\text{s}}} \right\}, \\ m'_{\pm}(x) &= \mp \frac{xN_0}{4N_{\text{s}}\rho_k}, \\ {\rho'_k}^2 &= \frac{N_0}{4N_{\text{s}}\rho_k^2}. \end{aligned}$$

From the definition in Section II, $\text{ASNR}_k = \frac{2N_{\text{s}}\rho_k^2}{N_0}$. If the ASNR_k is high enough, $N_{\varrho_k}(m'_{\pm}(x), {\rho'_k}^2)$ in (17) with a narrow shape behaves like a delta function. If the ASNR_k is low, $f(\varrho_k)$ with a relatively narrow shape behaves like a delta function at the mean value of ϱ_k. Therefore, the integral in (17) is approximated asymptotically by

$$\begin{aligned} & k'(x) \int_0^{\infty} N_{\varrho_k}(m'_{\pm}(x), {\rho'_k}^2) f(\varrho_k) d\varrho_k \\ & \approx \begin{cases} k'(x) \cdot [f'(m'_{\pm}(x)) & \\ \quad + \varpi N_{\psi}(m'_{\pm}(x), {\rho'_k}^2)] & \text{high } \text{ASNR}_k \\ k'(x) \cdot N_{\mathbb{E}\{\varrho_k\}}(m'_{\pm}(x), {\rho'_k}^2) & \text{low } \text{ASNR}_k. \end{cases} \end{aligned} \qquad (18)$$

Note that either $f'(m'_+(x))$ or $f'(m'_-(x))$ equals zero because $\varrho_k \geq 0$, $f'(|m'_+(x)|) \leq \max_{\varrho_k} N_{\varrho_k}(|m'_+(x)|, {\rho'_k}^2) = \sqrt{2N_{\text{s}}\rho_k^2/\pi N_0}$ is true for any $|m'_+(x)|$ when ASNR_k is high because of the delta function behavior of $N_{\varrho_k}(m'_{\pm}(x), {\rho'_k}^2)$, and $\varpi N_{\psi}(m'_{\pm}(x), {\rho'_k}^2) \leq \varpi \sqrt{2N_{\text{s}}\rho_k^2/\pi N_0}$. For the large ASNR_k situation, either $\frac{C^2(k)N_0}{N_{\text{s}}}$ or $\frac{D^2(k)N_0}{N_{\text{s}}}$ is large, and the other is close to zero, depending on the transmitted bit. Suppose $\frac{C^2(k)N_0}{N_{\text{s}}}$ is the large one whose mean is $4 + \frac{16N_{\text{s}}\rho_k^2}{N_0}$, then

$$k'(C(k)) \gg f'(|m'_{\pm}(C(k))|) + \varpi N_{\psi}(m'_{\pm}(C(k)), {\rho'_k}^2),$$

in which $C(k)$ is substituted for x. By applying the above inequality to the high ASNR_k case in (18) and (17), the suboptimal rule approximating (9) is

$$\sum_{k=0}^{K-1} \ln\{k'(C(k))\} \underset{-1}{\overset{1}{\gtrless}} \sum_{k=0}^{K-1} \ln\{k'(D(k))\},$$

which is equivalent to

$$\sum_{k=0}^{K-1} C_{\text{R}}(k) C_{\text{D}}(k) \underset{-1}{\overset{1}{\gtrless}} 0. \qquad (19)$$

For the low ASNR_k case, by substituting (18) into (17) and eliminating terms which have no effect on the decision, the suboptimal rule approximating (9) is

$$\sum_{k=0}^{K-1} \ln\{\cosh(\mathbb{E}\{\alpha_k\} C(k))\} \underset{-1}{\overset{1}{\gtrless}} \sum_{k=0}^{K-1} \ln\{\cosh(\mathbb{E}\{\alpha_k\} D(k))\}. \qquad (20)$$

Both $\ln(\cdot)$ and $\cosh(\cdot)$ are nonlinear strictly monotonic increasing functions. Because $\cosh(\cdot)$ is even, the function $\ln(\cosh(\cdot))$ is also even, and

$$\ln\{\cosh(y)\} \cong \ln\{e^{|y|}\} - \ln 2 = |y| - \ln 2. \qquad (21)$$

Equation (20) is now simplified by applying (21)

$$\sum_{k=0}^{K-1} \mathbb{E}\{\alpha_k\}|C_{\mathrm{R}}(k)+C_{\mathrm{D}}(k)| \underset{-1}{\overset{1}{\gtrless}} \sum_{k=0}^{K-1} \mathbb{E}\{\alpha_k\}|C_{\mathrm{R}}(k)-C_{\mathrm{D}}(k)|, \tag{22}$$

where $|C_{\mathrm{R}}(k)+C_{\mathrm{D}}(k)|$ and $|C_{\mathrm{R}}(k)-C_{\mathrm{D}}(k)|$ are received information of bit b_0 which are weighted by the mean value of the amplitude of path signals. This suboptimal decision rule can be simplified further to

$$\sum_{k=0}^{K-1} |C_{\mathrm{R}}(k)+C_{\mathrm{D}}(k)| \underset{-1}{\overset{1}{\gtrless}} \sum_{k=0}^{K-1} |C_{\mathrm{R}}(k)-C_{\mathrm{D}}(k)| \tag{23}$$

because multiplying the prior information $\mathbb{E}\{\alpha_k\}$ at low ASNR_k does not improve the bit error probability much which will be seen in Section VI.

For the performance analysis, a closed-form evaluation of the suboptimal receiver in (19) can be obtained by using Appendix 9A in [17]. With the assumption that K is even, and by defining $A = B = 0$, $C = 1/2$, $L = K/2$, $X_n = C_{\mathrm{R}}(n) + jC_{\mathrm{R}}(n+\frac{K}{2})$, and $Y_n = C_{\mathrm{D}}(n) + jC_{\mathrm{D}}(n+\frac{K}{2})$ for $n = 0, 1, \ldots, L-1$, the left-hand side of (19), which is equal to $\frac{1}{2}\sum_{n=0}^{L-1}(X_n^{\mathrm{h}}Y_n + Y_n^{\mathrm{h}}X_n)$ with X_n^{h} denoting the complex conjugate transpose of X_n, can be represented in the same form as (9A.1) in [17]. The means of $C_{\mathrm{R}}(k)$ and $C_{\mathrm{D}}(k)$ are $N_{\mathrm{s}}p_k\alpha_k$ and $b_0N_{\mathrm{s}}p_k\alpha_k$, their variances are both $\frac{N_{\mathrm{s}}N_0}{2}$ which are independent of k, and any two of $\{C_{\mathrm{R}}(k), C_{\mathrm{D}}(k)\}_k$ are uncorrelated. Assuming $b_0 = 1$, the values of parameters a and b defined in [17] are computed as $a = 0$ and $b = \sqrt{\frac{2N_{\mathrm{s}}\sum_{k=0}^{K-1}\alpha_k^2}{N_0}} = \sqrt{\frac{E_{\mathrm{b}}}{N_0}}$ where E_{b}, the realized bit energy, is a random variable. The BEP conditioned on $\frac{E_{\mathrm{b}}}{N_0}$ is acquired by substituting a and b into (9A.15) in [17]

$$P_{\mathrm{bit}}(\alpha_0, \ldots, \alpha_{K-1}) = \frac{1}{2} + \frac{1}{2^{K-1}} \sum_{l=1}^{K/2} \binom{K-1}{\frac{K}{2}-l} \left[Q_l\left(0, \sqrt{\frac{E_{\mathrm{b}}}{N_0}}\right) - Q_l\left(\sqrt{\frac{E_{\mathrm{b}}}{N_0}}, 0\right)\right], \tag{24}$$

where $Q_l(\zeta, \varsigma)$ is a Marcum Q-function. Because $Q_l(b, 0) = 1$ for all l, b, and

$$Q_l(0, b) = \sum_{n=0}^{l-1} \exp\left(-\frac{b^2}{2}\right) \frac{(b^2/2)^n}{n!}$$

if l is an integer, (24) can be simplified further to

$$P_{\mathrm{bit}}(\alpha_0, \ldots, \alpha_{K-1}) = \frac{1}{2^{K-1}} \sum_{l=1}^{K/2} \binom{K-1}{\frac{K}{2}-l} \sum_{n=0}^{l-1} \frac{1}{n!} \exp\left(-\frac{E_{\mathrm{b}}}{2N_0}\right) \left(\frac{E_{\mathrm{b}}}{2N_0}\right)^n. \tag{25}$$

In Section VI, Figure 5-8 show the fit of these analytical results and simulations. The closed-form solution of the average BEP can be acquired if $\mathbb{E}\left\{\exp\left(-\frac{E_{\mathrm{b}}}{2N_0}\right)\left(\frac{E_{\mathrm{b}}}{2N_0}\right)^n\right\}$ can be calculated, i.e., the moment generating function of $\frac{E_{\mathrm{b}}}{2N_0}$ exists.

A. Rayleigh Path Strength Models

The log-likelihood function (12) is a function of $w_{\mathrm{R}}(k)x^2$, and x could be $C(k)$ or $D(k)$. Using $x = C(k)$ as an example, without the receiver noise, $C(k)$ is equal to zero when $b_0 = -1$. Therefore, with moderate or high $\mathrm{RSNR}_k = 2N_{\mathrm{s}}\alpha_k^2/N_0$, $C(k)$ and also $w_{\mathrm{R}}(k)C^2(k)$ should be close to zero for $b_0 = -1$, and should have significant positive values for $b_0 = 1$. When $a \cong 1$ and the value of $w_{\mathrm{R}}(k)C^2(k)$ is large (i.e., RSNR_k is large and $b_0 = 1$), $L_k(C(k))$ can be approximated by

$$L_k(C(k)) \cong \frac{w_{\mathrm{R}}(k)C^2(k)}{2} \tag{26}$$

(see Appendix I). This approximation is also verified by Figure 3. For small RSNR_k or $b_0 = -1$ which produces small $w_{\mathrm{R}}(k)C^2(k)$, this approximation is not so precise. It is worth noting that when the value of a decreases, the probability that RSNR_k is small even with high ASNR_k and $b_0 = 1$ increases. High ASNR_k (or SNR_k) with small a can make the approximation in (26) deviate more from $L_k(C(k))$ because of the term $\left(\frac{1-a}{a}\right)(1+SNR_k)\exp\left(-\frac{w_{\mathrm{R}}(k)C^2(k)}{2}\right)$, and this is shown in Figure 3. Similar arguments and conclusions apply to (12) for $x = D(k)$.

By using the approximation in (26), the logarithm term in (12) is abandoned, and the suboptimal receiver is simplified to

$$\sum_{k=0}^{K-1} w_{\mathrm{R}}(k)C_{\mathrm{R}}(k)C_{\mathrm{D}}(k) \underset{-1}{\overset{1}{\gtrless}} 0. \tag{27}$$

(Rayleigh suboptimal receiver 1)

For a large SNR_k, approximation for $w_{\mathrm{R}}(k)$ also exists

$$w_{\mathrm{R}}(k) = \frac{\sigma_k^2}{1+SNR_k} \cong \frac{\sigma_k^2}{SNR_k} \cong \frac{N_0}{4N_{\mathrm{s}}},$$

which is a constant and does not have any effect. Then the decision rule in (27) is further reduced to

$$\sum_{k=0}^{K-1} C_{\mathrm{R}}(k)C_{\mathrm{D}}(k) \underset{-1}{\overset{1}{\gtrless}} 0 \tag{28}$$

(Rayleigh suboptimal receiver 2)

which is the same as (19) and the generalized likelihood ratio test (GLRT) receiver for a UWB TR system in [9].

The transmitted bit is the phase difference of the reference pulse and data pulse. Without receiver noise, the polarity of $C_{\mathrm{R}}(k)C_{\mathrm{D}}(k)$ for all k should be the same and is the transmitted bit. It is possible that the polarity of any $C_{\mathrm{R}}(k)C_{\mathrm{D}}(k)$ could differ from the transmitted bit because of the receiver noise, but the error probability decreases as the ASNR_k and RSNR_k increase. Therefore, we should give $C_{\mathrm{R}}(k)C_{\mathrm{D}}(k)$ different weights for different k according to both the *a priori* information and received information in the k^{th} path. For the weighted suboptimal detection in (27), we discard the information of RSNR and a part of ASNR, which is included in the logarithm term in (12), in order to reduce the receiver complexity. From Figure 3, this should have a small effect upon the BEP performance for a close to 1, or moderate and small a along

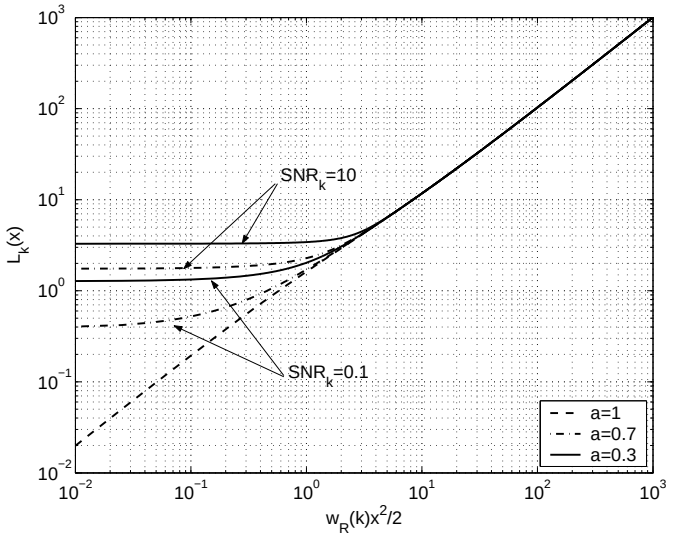

Fig. 3. $\frac{w_{\rm R}(k)x^2}{2}$ versus $L_k(x)$ for $k = 0, 1, \ldots, K-1$.

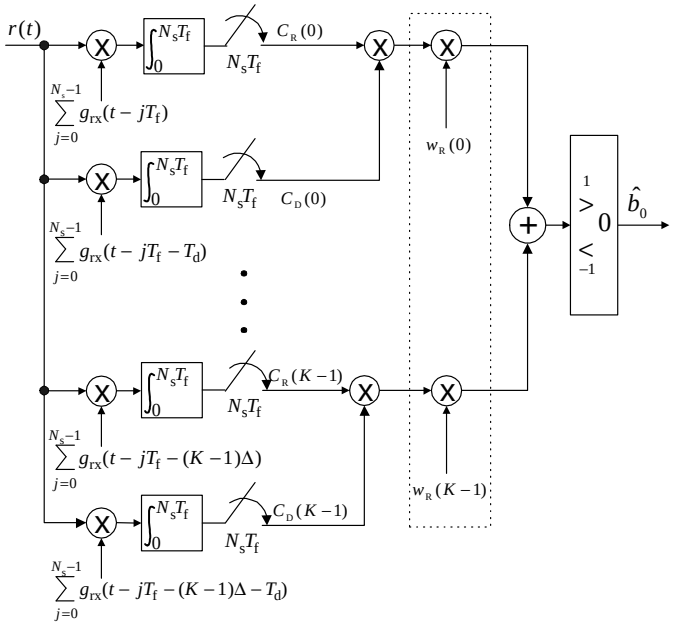

Fig. 4. The block diagram of ALRT suboptimal receivers described in (27) and (28) with Rayleigh path strength models.

with small ASNR. The weights for $\{C_{\rm R}(k)C_{\rm D}(k)\}_{k=0}^{K-1}$, which are $\{w_{\rm R}(k)\}_{k=0}^{K-1}$, can be generated according to the *a priori* knowledge in advance, and stored in the receiver. Since $w_{\rm R}(k)$ is an increasing function in σ_k^2, $C_{\rm R}(k)C_{\rm D}(k)$ gets a large weight if the average energy of an arrival in the $k^{\rm th}$ path is large.

In (28), no *a priori* information is used, and the receiver makes decision only according to the received information. The block diagram of the suboptimal receiver in (27) is shown in Figure 4, and the structure described in (28) is also drawn in the same figure except the multiplications by weights $\{w_{\rm R}(k)\}_{k=0}^{K-1}$ in the dotted box are removed.

The BEP of using the suboptimal decision rule in (27) conditioned on a channel realization can be computed by utilizing the result in [21]. Define

$$\begin{aligned} X_k = X_{{\rm R}k} + jX_{{\rm I}k} &\triangleq \sqrt{w_{\rm R}(2k-2)}C_{\rm R}(2k-2) \\ &+ j\sqrt{w_{\rm R}(2k-1)}C_{\rm R}(2k-1), \end{aligned}$$

$$\begin{aligned} Y_k = Y_{{\rm R}k} + jY_{{\rm I}k} &\triangleq \sqrt{w_{\rm R}(2k-2)}C_{\rm D}(2k-2) \\ &+ j\sqrt{w_{\rm R}(2k-1)}C_{\rm D}(2k-1), \end{aligned}$$

for $k = 1, 2, \ldots, \frac{K}{2}$ assuming K is even which can be easily produced by adding an additional path with zero magnitude if necessary. The variance and covariance of $X_{{\rm R}k}$, $X_{{\rm I}k}$, $Y_{{\rm R}k}$, and $Y_{{\rm I}k}$ can therefore be calculated which satisfy (1) and (2) in [21] except that

$$\mathbb{V}{\rm ar}\{X_{{\rm R}k}\} \neq \mathbb{V}{\rm ar}\{X_{{\rm I}k}\}, \quad \mathbb{V}{\rm ar}\{Y_{{\rm R}k}\} \neq \mathbb{V}{\rm ar}\{Y_{{\rm I}k}\},$$

where $\mathbb{V}{\rm ar}\{X_{{\rm R}k}\} = \mathbb{V}{\rm ar}\{Y_{{\rm R}k}\} = \frac{1}{2}N_{\rm s}N_0 w_{\rm R}(2k-2)$ and $\mathbb{V}{\rm ar}\{X_{{\rm I}k}\} = \mathbb{V}{\rm ar}\{Y_{{\rm I}k}\} = \frac{1}{2}N_{\rm s}N_0 w_{\rm R}(2k-1)$. Because of the dense UWB environment which makes $w_{\rm R}(2k-2) \cong w_{\rm R}(2k-1)$, the relationships in (1) and (2) in [21] are still approximately true. The effect of this approximation on evaluating the suboptimal receiver structure (27) is little which will be seen in Section VI. Let $\mathbf{v} = [X_1, Y_1, X_2, Y_2, \ldots, X_{K/2}, Y_{K/2}]^{\rm t}$, and

$$\mathbf{Q} = \frac{1}{2}\begin{bmatrix} H & 0 & . & . & 0 \\ 0 & H & 0 & . & 0 \\ . & 0 & . & . & . \\ . & . & . & . & 0 \\ 0 & . & . & 0 & H \end{bmatrix}$$

where

$$\mathbf{H} = \begin{bmatrix} 0 & 1 \\ 1 & 0 \end{bmatrix},$$

then

$$\Theta = \mathbf{v}^{\rm h}\mathbf{Q}\mathbf{v} \underset{-1}{\overset{1}{\gtrless}} 0$$

is equal to (27).

Let $\bar{\mathbf{v}}$ and $\mathbf{L}$ denote the mean vector and covariance matrix of $\mathbf{v}$ and assume $b_0 = 1$, the characteristic function of Θ can be written in this form

$$\phi(jt|b_0 = 1) = \prod_{k=1}^{K} \frac{\exp\{\frac{jt\lambda_k|d_k|^2}{1-jt\lambda_k}\}}{1-jt\lambda_k}, \tag{29}$$

where λ_k are the eigenvalues of $\mathbf{LQ}$, and

$$d_k = \begin{cases} \sqrt{\frac{4N_{\rm s}}{N_0}}\frac{\sqrt{w_{\rm R}(k-1)}p_{k-1}\alpha_{k-1} + j\sqrt{w_{\rm R}(k)}p_k\alpha_k}{\sqrt{w(k-1)+w(k)}} & k \text{ is odd} \\ 0 & k \text{ is even} \end{cases}$$

are computed using the methods in [21]. By defining $\xi_m = \frac{N_{\rm s}N_0}{4}[w_{\rm R}(2m-2) + w_{\rm R}(2m-1)] \geq 0$ for $m = 1, 2, \ldots, \frac{K}{2}$, the eigenvalues are

$$\lambda_l = \xi_{\frac{l+1}{2}}, \quad \lambda_{l+1} = -\xi_{\frac{l+1}{2}}$$

for $l = 1, 3, 5, \ldots, K-1$. The characteristic function of Θ by substituting λ_k and d_k into (29) and setting $z = jt$ is

$$\phi(z|b_0 = 1) = \left[\prod_{k=1}^{K/2} \frac{\frac{-1}{\xi_k}\exp\{\frac{z\xi_k|d_{2k-1}|^2}{1-z\xi_k}\}}{z - \frac{1}{\xi_k}}\right]\left[\prod_{k=1}^{K/2}\frac{\frac{1}{\xi_k}}{z+\frac{1}{\xi_k}}\right].$$

Knowing the characteristic function $\phi(z|b_0 = 1)$, the probability density function of Θ given $b_0 = 1$ is

$$f(\theta|b_0 = 1) = \frac{1}{2\pi j}\int_{-j\infty}^{j\infty} G(z)dz,$$

where

$$G(z) = \exp(-z\theta)\phi(z|b_0 = 1).$$

By defining $z_k = \frac{1}{\xi_k}$ for $k = 1, 2, \ldots, \frac{K}{2}$, the poles of $G(z)$ are $\pm z_k$ which are all simple poles. The bit error probability is

$$P_{\rm b} = \int_{-\infty}^{0} f(\theta|b_0 = 1)d\theta = \sum_{k=1}^{K/2}\int_{-\infty}^{0} \operatorname*{Res}_{z=-z_k} G(z)d\theta \quad (30)$$

due to the symmetry of the transmitted bit and receiver noise, as well as the claim in Appendix III. The residue of $G(z)$ at $-z_k$ is

$$\operatorname*{Res}_{z=-z_k} G(z) = G(z)(z + z_k)|_{z=-z_k}. \quad (31)$$

The BEP conditioned on one channel realization by substituting (31) into (30) is

$$P_{\rm b} = \frac{1}{2}\sum_{k=1}^{K/2}\exp\{-\frac{1}{2}|d_{2k-1}|^2\}\prod_{\substack{n=1\\ n\neq k}}^{K/2}\frac{\exp\left\{\frac{-\xi_n|d_{2n-1}|^2}{(\xi_k+\xi_n)}\right\}}{1-\left(\frac{\xi_n}{\xi_k}\right)^2}, \quad (32)$$

where d_l are functions of $\alpha_0, \alpha_1, \ldots, \alpha_{K-1}$.

B. Lognormal Path Strength Models

Suppose that $N = 1$ in the Hermite-Gauss approximation (15) is adopted for which $x_1 = 0$, $h(1) = 1$, and $w_1 = 1$. The log-likelihood function (16) is reduced and equivalent to

$$L_k(x) \equiv \ln\left\{\exp\left(-\frac{2N_{\rm s}}{N_0}w_{\rm L}^2(k)\right)\cosh(w_{\rm L}(k)x) + \frac{1-a}{a}\right\} \quad (33)$$

by discarding the constant $\ln(a)$ where $w_{\rm L}(k)$ is the prior information, i.e., the mean value of the amplitude of an arrival in the $k^{\rm th}$ path component, and $x = C(k)$ or $x = D(k)$. From the definition of $w_{\rm L}(k)$, $C(k)$ and $D(k)$, without receiver noise, $w_{\rm L}(k)C(k)$ is proportional to the ratio of the energy of the $k^{\rm th}$ multipath signal component to the noise power spectral density when $b_0 = 1$, and should be equal to zero when $b_0 = -1$. A similar argument can be applied to $w_{\rm L}(k)D(k)$. The second term in the braces in (33) is equal or close to zero when a is equal or close to one, then

$$L_k(x) \cong -\frac{2N_{\rm s}}{N_0}w_{\rm L}^2(k) + \ln\{\cosh(w_{\rm L}(k)x)\}. \quad (34)$$

By assuming a dense environment (a is close to 1) and adopting the approximation in (21), a suboptimal decision rule simplified from (33) is

$$\sum_{k=0}^{K-1} w_{\rm L}(k)|C_{\rm R}(k) + C_{\rm D}(k)| \underset{-1}{\overset{1}{\gtrless}} \sum_{k=0}^{K-1} w_{\rm L}(k)|C_{\rm R}(k) - C_{\rm D}(k)| \quad (35)$$

(lognormal suboptimal receiver 1)

which is the same as (22), and could deviate from (33) when a is small.

If the weights in (35) are eliminated to simplify the receiver structure further, the second suboptimal receiver structure becomes

$$\sum_{k=0}^{K-1} |C_{\rm R}(k) + C_{\rm D}(k)| \underset{-1}{\overset{1}{\gtrless}} \sum_{k=0}^{K-1} |C_{\rm R}(k) - C_{\rm D}(k)| \quad (36)$$

(lognormal suboptimal receiver 2)

which uses the received information only to make a decision, and is the same as (23). If there is only one path, i.e., $K = 1$, the decision regions of rules (9), (27), (28), (35) and (36) are all the same. Let the horizontal axis represent $C_{\rm R}(0)$ and the vertical axis represent $C_{\rm D}(0)$, we say that the transmitted bit is equal to 1 if the value of $(C_{\rm R}(0), C_{\rm D}(0))$ falls in quadrant one and three, and the transmitted bit is equal to -1 otherwise.

V. Cross-correlation Receivers and Comparisons with ALRT Suboptimal Receivers

Although those decision rules derived in Section III and IV have different optimal and suboptimal criteria, they all need a correlation operation for each multipath component to generate sufficient statistics $\{C_{\rm R}(k)\}_{k=0}^{K-1}$ and $\{C_{\rm D}(k)\}_{k=0}^{K-1}$ for detection. The more paths we have, the more correlation operations we need before the ADC. Because of the fine-time resolution capability a UWB signal has, it can resolve many multipath components, i.e., the number K is large. Therefore, the main reason that a transmitted reference method was proposed for use with a UWB system is to simplify receiver structures rather than to achieve optimal performance. The concept was to improve the performance with limited receiver complexity.

UWB TR systems employing *ad hoc* conventional cross-correlation receivers have been discussed widely [7]-[9]. This receiver correlates the received data-modulated waveform with the reference waveform, which is received $T_{\rm d}$ seconds earlier, to capture all the energy in the received signal, and sums the $N_{\rm s}$ correlator outputs that are affected by a single data bit (post-detection combining) to be the decision statistic. Since the time separation of the reference and data pulses are fixed to $T_{\rm d}$, the delay mechanism in the correlator can be implemented by a transmission line, a passive device, or an active device. In addition, because the correlation operation is done before the ADC, the sampling frequency of the ADC can also be reduced. For a cross-correlation receiver, received signals are passed through a bandpass filter before the correlation operation to reduce the incoming noise power, and resulting filtered signals and noises are marked by $\hat{(\cdot)}$. The decision rule of b_0 using conventional cross-correlation receivers is

$$D_{\rm c} = \sum_{j=0}^{N_{\rm s}-1}\int_{jT_{\rm f}+T_{\rm d}}^{jT_{\rm f}+T_{\rm d}+T_{\rm mds}} \hat{r}(t - T_{\rm d})\hat{r}(t)dt \underset{-1}{\overset{1}{\gtrless}} 0. \quad (37)$$

We assume in this paper that the power spectral density $S_n(f)$ of the noise $n(u, t)$ satisfies the white noise approximation, namely $S_n(f)|G_{\rm rx}(f)|^2 \cong \frac{N_0}{2}|G_{\rm rx}(f)|^2$, where $G_{\rm rx}(f)$ is the Fourier transform of $g_{\rm rx}(t)$. The BEP of this conventional

cross-correlation receiver was computed under the assumption of an ideal bandpass filter and the application of the orthonormal expansions in [19] and [20]. The result is written here

$$P_{\text{bit}}^{\text{c}} = \frac{1}{2^{2N_{\text{s}}B_{\text{w}}T_{\text{mds}}-1}} \sum_{l=1}^{N_{\text{s}}B_{\text{w}}T_{\text{mds}}} \binom{2N_{\text{s}}B_{\text{w}}T_{\text{mds}}-1}{N_{\text{s}}B_{\text{w}}T_{\text{mds}}-l} \times \sum_{n=0}^{l-1} \frac{1}{n!} \exp\left(-\frac{\hat{E}_{\text{b}}}{2N_0}\right)\left(\frac{\hat{E}_{\text{b}}}{2N_0}\right)^n, \quad (38)$$

where $\hat{E}_{\text{b}} = 2N_{\text{s}}\int_0^{T_{\text{mds}}} \hat{g}^2(t)dt$ is the filtered bit energy which depends on the channel realization, and B_{w} is the one-sided receiver bandwidth.

One method to improve the BEP performance of the conventional cross-correlation receiver is to average (or accumulate) the N_{s} reference waveforms in one bit time to reduce the noise in the template, and then data detection proceeds with this noise reduced template (pre-detection combining). The decision rule of b_0 using this average cross-correlation receiver is

$$D_{\text{a}} = \sum_{j=0}^{N_{\text{s}}-1} \int_{jT_{\text{f}}+T_{\text{d}}}^{jT_{\text{f}}+T_{\text{d}}+T_{\text{mds}}} \hat{r}(t) \sum_{i=-j}^{N_{\text{s}}-1-j} \hat{r}(t+iT_{\text{f}}-T_{\text{d}})dt \underset{-1}{\overset{1}{\gtrless}} 0, \quad (39)$$

and the BEP given one channel realization is computed using orthonormal expansions in [19] and [20] which is

$$P_{\text{bit}}^{\text{a}} = \frac{1}{2^{2B_{\text{w}}T_{\text{mds}}-1}} \sum_{l=1}^{B_{\text{w}}T_{\text{mds}}} \binom{2B_{\text{w}}T_{\text{mds}}-1}{B_{\text{w}}T_{\text{mds}}-l} \times \sum_{n=0}^{l-1} \frac{1}{n!} \exp\left(-\frac{\hat{E}_{\text{b}}}{2N_0}\right)\left(\frac{\hat{E}_{\text{b}}}{2N_0}\right)^n. \quad (40)$$

The average bit error probability of the conventional and average cross-correlation receivers can be obtained if $\mathbb{E}\{\exp(-\frac{\hat{E}_{\text{b}}}{2N_0})(\frac{\hat{E}_{\text{b}}}{2N_0})^n\}$ exits for all n, i.e., the moment generating function of $\frac{\hat{E}_{\text{b}}}{2N_0}$ exists.

A UWB system usually transmits a bit $N_{\text{s}} > 1$ times to achieve the appropriate signal energy to make a correct decision. In addition, often an application environment in which the TR method is preferred has a large number of paths, namely the channel delay spread T_{mds} is not short. Therefore, the noise dimension is large enough to conclude that this sum of integrals of the product of two Gaussian random processes is itself approximately Gaussian by central limit theorem arguments. Only first and second moments under this Gaussian assumption are required to evaluate the BEP, and the results which were computed in [9] are rewritten here

$$P_{\text{bit}}^{\text{c}} \cong Q\left(\left[\left(\frac{2N_0}{\hat{E}_{\text{b}}}\right) + 2B_{\text{w}}N_{\text{s}}T_{\text{mds}}\left(\frac{N_0}{\hat{E}_{\text{b}}}\right)^2\right]^{-\frac{1}{2}}\right), \quad (41)$$

$$P_{\text{bit}}^{\text{a}} \cong Q\left(\left[\left(\frac{2N_0}{\hat{E}_{\text{b}}}\right) + 2B_{\text{w}}T_{\text{mds}}\left(\frac{N_0}{\hat{E}_{\text{b}}}\right)^2\right]^{-\frac{1}{2}}\right). \quad (42)$$

The resolvable multipath assumption (used in the development of (9)) is not necessary for the conventional and average cross-correlation receivers.

Comparing (41) and (42), an average cross-correlation receiver can reduce the noise power in the noise $\times$ noise term by a factor of N_{s}. The problem is the averaging process might not be easily implemented because of restricted receiver complexity, namely be implemented using analog devices before the correlator. In a multiple access environment, a hopping sequence is applied to each user to avoid catastrophic collisions [1]. The positions of reference pulses in different frames varies with the hopping sequence. In order to average N_{s} received reference waveforms, we need a delay mechanism to put those N_{s} references together. Even in a single user environment without a hopping sequence, when N_{s} is large, the number and length of delays make the implementation impossible. If the average process is implemented using digital techniques, then we need an ADC with high-sampling-frequency to sample and quantize the received signal. In this case, since the signals have already been digitized, there is no need to restrict the receiver structure as a cross-correlation receiver, and all kinds of digital signal processing schemes can be used to improve the BEP performance. Either in a single user or a multiple access environment, the time separation is fixed to T_{d}. This means the structure of the conventional cross-correlation receiver remains the same in both cases.

It is important to discuss the similarities between *ad hoc* cross-correlation receivers and the ALRT suboptimal receiver in (19). Under the resolvable multipath assumption, the set of correlator templates $\{g_{\text{rx}}(t-k\Delta)\}_{k=0}^{K-1}$ is a complete set of orthonormal basis functions for the received signal $g(t)$. The suboptimal receiver in (19) therefore obtains all the energy in the received signal, as does the average cross-correlation receiver (which can be shown by expressing $g(t)$ using the orthonormal expansions). For the average cross-correlation receiver, the incoming receiver noise has dimension $2B_{\text{w}}T_{\text{mds}}$. On the other hand, the suboptimal receiver (19) has noise dimension $K < 2B_{\text{w}}T_{\text{mds}}$ in the resolvable multipath conditions. Therefore, the receiver in (19) performs better than the average cross-correlation receiver by capturing the same signal energy with less incoming receiver noise. Suppose now additional $2B_{\text{w}}T_{\text{mds}} - K$ orthonormal functions, which along with the original K basis functions expanding the filtered noise space, are put in the orthonormal basis set. The receiver in (19) with these $2B_{\text{w}}T_{\text{mds}}$ orthonormal functions as correlator templates is equivalent to the average cross-correlation receiver. But note that the additional $2B_{\text{w}}T_{\text{mds}} - K$ orthonormal functions only capture noise.

The receiver in (19) and the average cross-correlation receiver acquire the multipath diversity with pre-detection combining. The conventional cross-correlation receiver acquires the multipath diversity through a post-detection combining. Investigating (38) and (40) or (41) and (42) indicates that for a specified $\hat{E}_{\text{b}}/N_0$, N_{s} is irrelevant to the BEP of an average cross-correlation receiver while the BEP of a conventional cross-correlation receiver varies with N_{s}. The effect of the noise $\times$ noise term depends on the energy in the template to the noise power ratio, and becomes more serious

when this value is low. This value for the average cross-correlation receiver is fixed for a specified $\hat{E}_{\rm b}/N_0$ because the signal energy in the reference waveforms in $N_{\rm s}$ frames is accumulated first before the correlation operation. For a conventional cross-correlation receiver and a specified $\hat{E}_{\rm b}/N_0$, because only one reference waveform serves as a template, the larger the $N_{\rm s}$ is, the smaller the energy in one reference pulse is. Therefore, the BEP performance becomes worse when $N_{\rm s}$ becomes larger. Pre-detection and post-detection combinations perform differently in *ad hoc* cross-correlation receivers. And the suboptimal receiver in (19), even with an extended orthonormal set to expand the noise space, is still not equivalent to the conventional cross-correlation receiver in (37).

VI. Numerical Results

The receiver structures we discussed above have nonlinear operations which make the theoretical BEP analysis difficult. Except for the receivers in (19), (27), (37) and (39), the BEPs of other receiver structures are evaluated by Monte Carlo simulations. In this section, we generate both Rayleigh and lognormal path strength models to test different receiver structures.

The single received pulse is a second derivative of a Gaussian pulse $g_{\rm rx}(t) = \frac{1}{c}[1-4\pi(\frac{t-\tau_1}{\tau})^2]\exp[-2\pi(\frac{t-\tau_1}{\tau})^2]$ for $t \in [0, 0.7]$ ns with $\tau = 0.2877$ ns and $\tau_1 = 0.35$ ns, and zero elsewhere. The constant c normalizes the energy in $g_{\rm rx}(t)$ to 1, and 97% of the received pulse's power is contained in 1-5GHz. Therefore, an ideal bandpass filter with 1-5GHz pass band is used in cross-correlation receivers, and $B_{\rm w} = 4$GHz. This 4GHz bandwidth might not be the optimal choice because decreasing the receiver bandwidth will reduce the signal energy but also reduce the incoming noise power. For both Rayleigh and lognormal environments, $\Delta = 0.7$ ns, $a = 1$, 0.7, and 0.3, $K = 84$, and the average power decay profile is assumed exponential with decay time constant $\Gamma = 8.5$ ns. The average power of the first multipath signal component Ω is chosen such that the average $E_{\rm b}/N_0$ ($\bar{E}_{\rm b}/N_0$) can achieve different values. For lognormal cases, $2N_{\rm s}a\sum_{k=0}^{K-1}\mathbb{E}[\alpha_k^2] = \bar{E}_{\rm b}$, and $\mathbb{E}[\alpha_k^2] = \Omega\exp(\frac{-k\Delta}{\Gamma})$. In addition, the standard deviation of $20\log(\alpha_k)$, σ, is equal to $4.8/\sqrt{2}$ for all k, and the mean of $20\log(\alpha_k)$ can be computed as $\mu_k = \frac{10\ln\Omega - 10k\Delta/\Gamma}{\ln 10} - \frac{\sigma^2\ln 10}{20}$. For Rayleigh models, $4N_{\rm s}a\sum_{k=0}^{K-1}\sigma_k^2 = \bar{E}_{\rm b}$, and $2\sigma_k^2 = \Omega\exp(\frac{-k\Delta}{\Gamma})$. These Rayleigh and lognormal channel models with root mean square delay spread around 7 ns represent small indoor environments.

In order to explain the BEP performance clearly, we name the decision rules in

- (9) with (12): ALRT Rayleigh receiver,
- (27): Rayleigh suboptimal receiver 1,
- (28): Rayleigh suboptimal receiver 2,
- (9) with (16): ALRT lognormal receiver with N,
- (35): lognormal suboptimal receiver 1,
- (36): lognormal suboptimal receiver 2,
- (37): conventional cross-correlation receiver,
- (39): average cross-correlation receiver.

In the simulations of the ALRT lognormal receiver, we tried $N = 1$, 2, 3, 4, 5, 6, 7, 8, 9, 10, 12, 16, and 20, and the simulated BEP results remain unchanged for $N \geq 8$. Besides, results from $N = 2$ to $N = 8$ are close. Therefore in performance figures, we only show the cases of $N = 1$, 2, and 8.

The differences of the BEP of conventional and average cross-correlation receivers evaluated by the formulas ((38) and (40)) and Gaussian approximation formulas ((41) and (42)) can not be distinguished in our simulation environments, thus only one result line for each kind of cross-correlation receivers is displayed in performance figures. This also indicates that the Gaussian approximation is good if the noise time$\times$bandwidth product is large enough. Performance figures showing that theoretical analyses and simulation results of the Rayleigh suboptimal receiver 1 and 2 agree with each other verify the programs.

The following figures show the bit error probability averaged over channel statistics, versus the average $E_{\rm b}/N_0$. Thus the value of the error probability is the observation in time varying channels over a long time. Suppose the channel is stationary during the observation, the BEP obtained could deviate from the curves shown in the figures, and should depend on that specific channel.

A. Rayleigh Environments v.s. Lognormal Environments

Figure 5 shows that the four best receivers in Rayleigh environments with $a = 1$ are the ALRT Rayleigh receiver, Rayleigh suboptimal receiver 1, and ALRT lognormal receivers with $N = 8$ and 2, which have nearly identical BEP performance. Hence the Rayleigh suboptimal receiver 1 is a better choice among these four receivers because of its simpler structure. ALRT lognormal receiver with $N = 1$ and lognormal suboptimal receiver 1 have slightly worse but competitive performance than the best, and the degradation occurs because only one term is used in the Hermite-Gauss integral (see (33)-(35)). It is expected that the performance of the Rayleigh suboptimal receiver 2 and lognormal suboptimal receiver 2 are worse because they discard *a priori* information about random channels. The lack of terms in the Hermite-Gauss integral also causes performance degradation in the lognormal suboptimal receiver 2.

Figure 6 shows the BEP performance in lognormal environments with $a = 1$. The five best performed receivers in turn are the ALRT lognormal receivers with $N = 8$ and 2, ALRT Rayleigh receiver, ALRT lognormal receivers with $N = 1$, and Rayleigh suboptimal receiver 1, and their BEPs are close. The performance of the lognormal suboptimal receiver 1 is only slightly worse than the best. Again, the Rayleigh and lognormal suboptimal receiver 2 perform worse than other receivers because of lack of *a priori* information about channels. The average and conventional cross-correlation receivers have 5dB and 10dB performance degradation respectively compared to the best performance for $N_{\rm s} = 10$ at BEP=1e-3.

Figure 5, 6 and 7 show that the Rayleigh suboptimal receiver 1 with an relatively easier-to-implement structure performs close to the optimal receiver in both Rayleigh and lognormal environments with normal to high multipath component

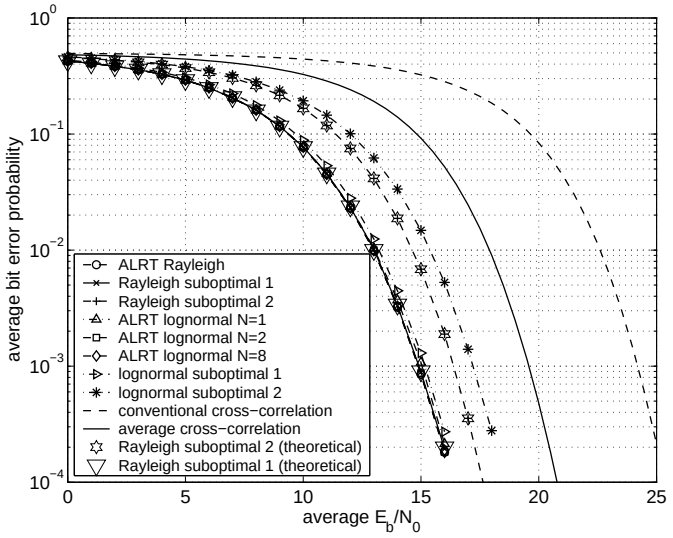

Fig. 5. Average bit error probabilities of different receiver structures for $N_s = 10$ in Rayleigh environments with $a = 1$.

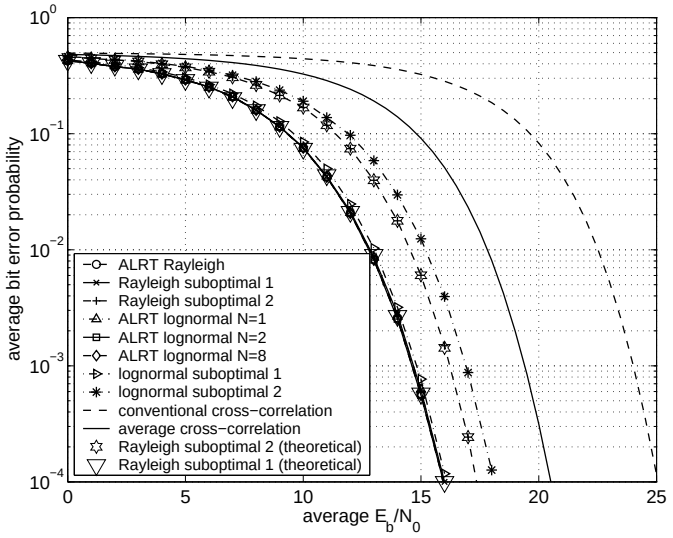

Fig. 6. Average bit error probabilities of different receiver structures for $N_s = 10$ in lognormal environments with $a = 1$.

arrival probability a. Figure 5 and 6 show that optimal ALRT receivers derived from Rayleigh and lognormal path strength models perform equally well in each other's environments. Different amplitude distributions have been proposed by different authors for UWB systems [10], [12], but these figures show that the BEP performance of an ALRT optimal receiver is irrelevant to path strength models.

B. Effects of Multipath Component Arrival Probability a

Figure 7 and 8 also show different receivers performing in Rayleigh environments but with $a = 0.7$ and 0.3. For a=0.7 and in the interested BEP range, we can see again that the ALRT Rayleigh receiver, ALRT lognormal receiver, and Rayleigh suboptimal receiver 1 almost perform equally well. The performance of other receivers is similar to the $a = 1$ case. But when a becomes small, this situation changes. In

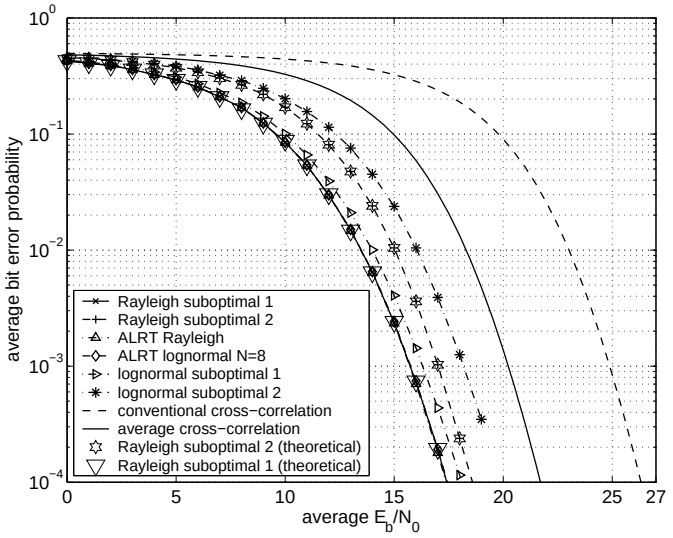

Fig. 7. Average bit error probabilities of different receiver structures for $N_s = 10$ in Rayleigh environments with $a = 0.7$.

Figure 8, ALRT Rayleigh and ALRT lognormal receivers still perform best, but the BEP of the Rayleigh suboptimal receiver 1 departs from them. As $\bar{E}_b/N_0$ increases, the performance of the Rayleigh and lognormal suboptimal receiver 1 approach that of the Rayleigh and lognormal suboptimal receiver 2, respectively. We can see from the figure that as $\bar{E}_b/N_0$ is large enough, the suboptimal receiver 2 even performs better than the suboptimal receiver 1.

The Rayleigh and lognormal suboptimal receiver 1 give each possible multipath signal component a weight according to *a priori* information which does not include the path existence probability a. As the value of a decreases, the probability of having an arrival in each time slot becomes small. It might happen that large weights are given to some time slots without arrivals. This weighting strategy can make the performance worse than without weighting. This observation is similar to the situation happening in the Rake reception. Maximal ratio combining (MRC) is optimal in maximum likelihood sense only if channel states are completely known. In reality, we have to estimate the channel and some estimation error can happen. When the estimation error increases, the performance of MRC and equal gain combining (EGC) become close, and EGC can eventually outperform MRC when the estimation error is large enough. Figure 5, 7, and 8 also show that for a specified $\bar{E}_b/N_0$, all the receivers perform worse in an environment with smaller a because of the uncertainty.

The observation we made in this subsection for Rayleigh environments with $a = 0.7$ and 0.3 also applies to lognormal environments .

C. Effects of N_s

In Figure 5-8, one bit is transmitted in $N_s = 10$ consecutive frames. For all ALRT optimal and suboptimal receivers as well as the average cross-correlation receiver, the value of N_s does not affect their BEPs because of the pre-detection combining. The effect of N_s on the conventional cross-correlation receiver is shown in these figures (conventional

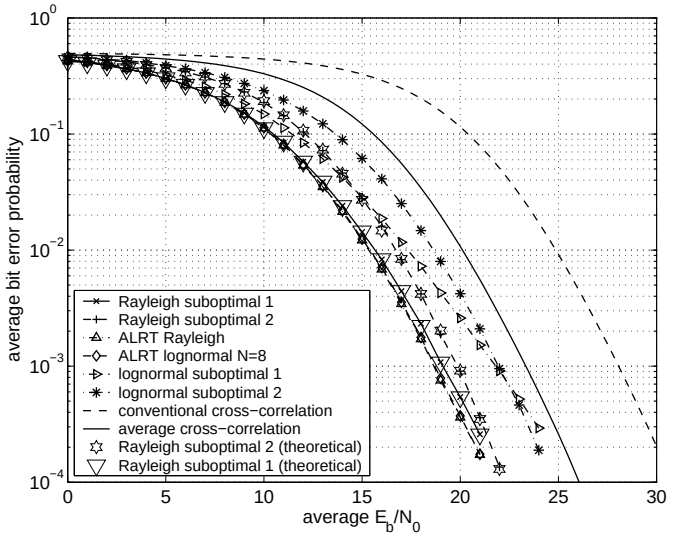

Fig. 8. Average bit error probabilities of different receiver structures for $N_s = 10$ in Rayleigh environments with $a = 0.3$.

cross-correlation receivers with $N_s = 1$ perform the same as average cross-correlation receivers) which illustrate that increasing N_s degrades the BEP. For $N_s = 10$ and 100, the receiver has 5dB and 10dB performance degradation compared to the $N_s = 1$ case at BEP=1e-3. And the conventional and average cross-correlation receivers are the same when $N_s = 1$. The signal energy to noise power ratio in a conventional cross-correlation receiver output is defined as

$$d^c_{SNR} = \left[\frac{2N_0}{\hat{E}_b} + 2B_w N_s T_{mds} \left(\frac{N_0}{\hat{E}_b} \right)^2 \right]^{-1},$$

and the BEP using Gaussian approximation in (41) is equal to $Q(\sqrt{d^c_{SNR}})$. For a given BEP, we can find a value y so that the BEP is achieved if $d^c_{SNR} = y$. By solving $d^c_{SNR} = y$, the required $\frac{\hat{E}_b}{N_0}$ is

$$\frac{\hat{E}_b}{N_0} = \frac{2B_w N_s T_{mds}}{\sqrt{1 + \frac{2B_w N_s T_{mds}}{y}} - 1} \cong \sqrt{2B_w N_s T_{mds} y}. \quad (43)$$

We can now see the effect of increasing N_s. For a specific BEP (or y), the required $\hat{E}_b/N_0$ approximately increases $10\log(\sqrt{n_2/n_1})$ dB for N_s increasing from n_1 to n_2. Figure 5-8 agree with this result.

It is worth to note that the BEP of cross-correlation receivers can be improved by applying some weighting functions before the integration, and the details are in [16] and [20].

D. Rayleigh Suboptimal Receiver 2 v.s. Average Cross-correlation Receiver

As in the discussion of conventional cross-correlation receivers in Subsection VI-C, the signal energy to noise power ratio in the decision statistic for the Rayleigh suboptimal receiver 2 is

$$d^R_{SNR} = \left[\frac{2N_0}{E_b} + K \left(\frac{N_0}{E_b} \right)^2 \right]^{-1}.$$

By using the same method, the required $\frac{E_b}{N_0}$ to achieve $d^R_{SNR} = y$ is

$$\frac{E_b}{N_0} \cong \sqrt{Ky}. \quad (44)$$

By comparing (43) and (44) with $N_s = 1$, $T_{mds} = 7K \times 10^{-10}$, and $\hat{E}_b \cong E_b$, the performance difference between the Rayleigh suboptimal receiver 2 and the average cross-correlation receiver is roughly $10\log(\sqrt{1.4B_w \times 10^{-9}}) = 3.7$ dB which is verified in Figures 5-8.

VII. Conclusion

This paper derives ALRT optimal and suboptimal receivers for UWB TR systems in both Rayleigh and lognormal environments, and shows the GLRT optimal receiver is one of the suboptimal receivers in ALRT sense by dropping the *a priori* information of channels. Performance results show that ALRT optimal receivers derived for Raleigh and lognormal path strength models can perform equally well in each other's environments, and the Rayleigh suboptimal receiver 1, which has a relatively simple receiver structure, performs close to the optimal one when the multipath component existence probability is normal to high. In a low path arrival probability environment, the performance of both Rayleigh and lognormal suboptimal receiver 1 becomes closer to and even worse than that of the Rayleigh and lognormal suboptimal receiver 2 as $\bar{E}_b/N_0$ increases. The *ad hoc* cross-correlation receivers perform worse than ALRT optimal and suboptimal receivers, and the BEP of the conventional cross-correlation receiver degrades as N_s increases for a fixed $\bar{E}_b/N_0$. The Rayleigh suboptimal receiver 2, by expanding the number of correlator templates, can be equivalent to the average cross-correlation receiver. Central limit theorem can help evaluate the BEP of cross-correlation receivers well by approximating the noise $\times$ noise term Gaussian distributed when the noise time$\times$bandwidth product is large.

Appendix I

When the value of $w_R(k)x^2$ is large and a is close to 1,

$$\begin{aligned} 1 - 2Q\left(\sqrt{w_R(k)x^2}\right) &\cong 1, \\ \exp\left(-\frac{w_R(k)x^2}{2}\right) &\cong 0, \\ \frac{1-a}{a} &\cong 0. \end{aligned}$$

With $1 + SNR_k$ being bounded, by substituting these approximations into (12),

$$\begin{aligned} L_k(x) &\cong \frac{w_R(k)x^2}{2} + \ln\left\{\sqrt{\frac{\pi w_R(k)x^2}{2}}\right\} \\ &\cong \frac{w_R(k)x^2}{2}. \end{aligned}$$

APPENDIX II

The nuisance parameter α_k in (10) is integrated first by inserting (6) and (11) into $f(\alpha_k)$. The integral (46) is derived by applying formula 3.462.5 in [15] to (45)

$$L_k(x) = \ln\left\{\int_{-\infty}^{\infty} f(p_k)\left[\int_0^{\infty}\frac{a\alpha_k}{\sigma_k^2}\exp\{p_k\alpha_k x - \alpha_k^2\left(\frac{2N_{\rm s}}{N_0}+\frac{1}{2\sigma_k^2}\right)\right\}d\alpha_k + (1+a)\Bigg]dp_k\right\} \tag{45}$$

$$= \ln\left\{\int_{-\infty}^{\infty}\left[\frac{a}{\sigma_k^2}\left(\frac{1}{\frac{4N_{\rm s}}{N_0}+\frac{1}{\sigma_k^2}}+\frac{p_k x}{\frac{4N_{\rm s}}{N_0}+\frac{1}{\sigma_k^2}}\times\sqrt{\frac{\pi}{\frac{2N_{\rm s}}{N_0}+\frac{1}{2\sigma_k^2}}}\exp\left(\frac{x^2}{\frac{8N_{\rm s}}{N_0}+\frac{2}{\sigma_k^2}}\right)\right)\right.\right. \tag{46}$$

$$\left.\left.\times Q\left(-\frac{p_k x}{2}\sqrt{\frac{2}{\frac{2N_{\rm s}}{N_0}+\frac{1}{2\sigma_k^2}}}\right)+(1-a)\right]f(p_k)dp_k\right\}$$

$$= \ln\left\{\int_{-\infty}^{\infty}\left\{\frac{aw_{\rm R}(k)}{\sigma_k^2}+\frac{ap_k x\sqrt{2\pi w_{\rm R}^3(k)}}{\sigma_k^2}\times\exp\left(\frac{x^2 w_{\rm R}(k)}{2}\right)Q\left(-p_k x\sqrt{w_{\rm R}(k)}\right)\right.\right.$$

$$\left.\left.+(1-a)\right\}\left(\frac{1}{2}\delta_{\rm D}(p_k-1)+\frac{1}{2}\delta_{\rm D}(p_k+1)\right)dp_k\right\}.$$

In the following integration of p_k using (5), (47) is simplified to (48) because $Q(-x) = 1 - Q(x)$ and $x[1 - 2Q(x\sqrt{w_{\rm R}(k)})] \geq 0$

$$L_k(x) = \ln\left\{\frac{aw_{\rm R}(k)}{\sigma_k^2}+\frac{ax\sqrt{2\pi w_{\rm R}^3(k)}}{2\sigma_k^2}\exp\left(\frac{x^2 w_{\rm R}(k)}{2}\right)\times\left[Q\left(-x\sqrt{w_{\rm R}(k)}\right)-Q\left(x\sqrt{w_{\rm R}(k)}\right)\right]+(1-a)\right\} \tag{47}$$

$$= \ln\left\{\frac{aw_{\rm R}(k)}{\sigma_k^2}+\frac{a\sqrt{2\pi w_{\rm R}^3(k)x^2}}{2\sigma_k^2}\exp\left(\frac{x^2 w_{\rm R}(k)}{2}\right)\times\left[1-2Q\left(\sqrt{w_{\rm R}(k)x^2}\right)\right]+(1-a)\right\}. \tag{48}$$

APPENDIX III

Claim 1:

$$\int_{-j\infty}^{j\infty} G(z)dz = 2\pi j\sum_{k=1}^{K/2}\operatorname*{Res}_{z=-z_k} G(z).$$

Proof: In Figure 9, the line from $(0,-jR)$ to $(0,jR)$ and C_R which comes back to $(0,-jR)$ compose of a positively oriented simple closed contour including all negative poles of $G(z)$ in it. It is directly from the Cauchy's residue theorem that

$$\int_{-jR}^{jR} G(z)dz + \int_{C_R} G(z)dz = 2\pi j\sum_{k=1}^{K/2}\operatorname*{Res}_{z=-z_k} G(z).$$

Next, we show that $\int_{C_R} G(z)dz$ tends to 0 as R tends to ∞. Let $z = z_{\rm R} + jz_{\rm I} \in C_R$, it is obvious that $|z| = R$, $|z_{\rm R}| \leq R$, and $z_{\rm R} \leq 0$. The absolute value of $G(z)$ is

$$|G(z)| = |\exp(-z\theta)|\prod_{k=1}^{K/2}\frac{\left|\exp\{\frac{z\xi_k|d_{2k-1}|^2}{1-z\xi_k}\}\right|}{\xi_k^2\left|z-\frac{1}{\xi_k}\right|\left|z+\frac{1}{\xi_k}\right|}$$

$$\leq |\exp(-z\theta)|\prod_{k=1}^{K/2}\frac{\left|\exp\{\frac{z\xi_k|d_{2k-1}|^2}{1-z\xi_k}\}\right|}{\xi_k^2\left(R-\frac{1}{\xi_k}\right)^2},$$

and the last inequality results from $|z-\frac{1}{\xi_k}| \geq ||z|-\frac{1}{\xi_k}| = R-\frac{1}{\xi_k}$ and $|z+\frac{1}{\xi_k}| \geq ||z|-\frac{1}{\xi_k}|$. For each k,

$$\left|\exp\{\frac{z\xi_k|d_{2k-1}|^2}{1-z\xi_k}\}\right| = \exp\{-|d_{2k-1}|^2\}\left|\exp\left\{\frac{|d_{2k-1}|^2(1-z_{\rm R}\xi_k)}{(1-z_{\rm R}\xi_k)^2+(z_{\rm I}\xi_k)^2}\right\}\right| \tag{49}$$

by using the fact that $|\exp\{ju\}| = 1$ for any real number u. In addition, $1 - 2z_{\rm R}\xi_k \geq 0$ because $z_{\rm R} \leq 0$ and $\xi_k > 0$ which results in

$$(1-z_{\rm R}\xi_k)^2 + (z_{\rm I}\xi_k)^2 = 1 - 2z_{\rm R}\xi_k + R^2\xi_k^2 \geq R^2\xi_k^2.$$

Therefore, (49) is reduced to

$$\left|\exp\{\frac{z\xi_k|d_{2k-1}|^2}{1-z\xi_k}\}\right| \leq \exp\left\{-|d_{2k-1}|^2+\frac{|d_{2k-1}|^2(1+R\xi_k)}{R^2\xi_k^2}\right\}.$$

Beside, for $\theta \in (-\infty, 0]$,

$$|\exp(-z\theta)| = \exp(-z_{\rm R}\theta) \leq 1.$$

Therefore,

$$\left|\int_{C_{\rm R}} G(z)dz\right| \leq \int_{C_{\rm R}}|G(z)|dz = \pi R|G(z)|$$

$$\leq \pi R\prod_{k=1}^{K/2}\frac{\exp\left\{-|d_{2k-1}|^2+\frac{|d_{2k-1}|^2(1+R\xi_k)}{R^2\xi_k^2}\right\}}{\xi_k^2\left(R-\frac{1}{\xi_k}\right)^2}$$

$$\to 0 \quad \text{as } R \text{ tends to } \infty.$$

■

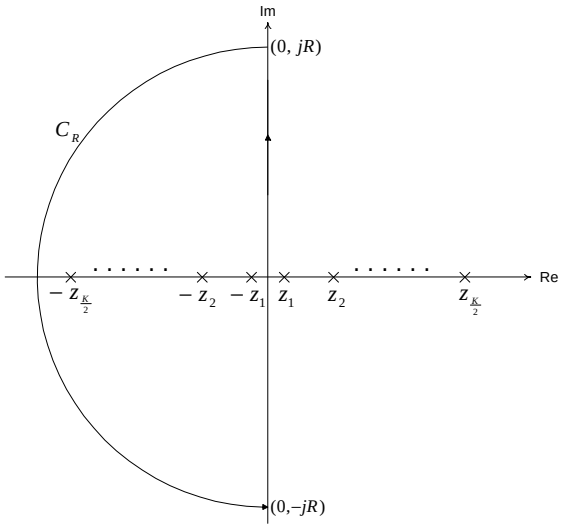

Fig. 9. Simple poles of $G(z)$.

REFERENCES

[1] R. A. Scholtz, "Multiple-access with time-hopping impulse modulation," *Proc. Military Communications Conf.*, vol. 2, Oct. 1993, pp. 447-450.

[2] M. Z. Win, R. A. Scholtz, "On the robustness of ultra-wide bandwidth signals in dense multipath environments," *IEEE Commun. Lett.*, vol. 2, pp. 51-53, Feb. 1998.

[3] M. Z. Win, R. A. Scholtz, "On the energy capture of ultra-wide bandwidth signals in dense multipath environments," *IEEE Commun. Lett.*, vol. 2, pp. 245-247, Sep. 1998.

[4] R. A. Scholtz, "The origins of spread-spectrum communications," *IEEE Trans. Commun.*, vol. 30, no. 5, pp. 822-854, May 1982.

[5] C. K. Rushforth, "Transmitted-reference techniques for random or unknown channels," *IEEE Trans. Inform. Theory*, Vol. 10, No. 1, pp. 39-42, Jan. 1964.

[6] R. A. Scholtz, *Coding for Adaptive Capability in Random Channel Communications*, Stanford Electronics Laboratories Report No. 6104-8, Dec. 1963.

[7] R. T. Hoctor and H. W. Tomlinson, "An overview of delay-hopped transmitted-reference RF communications," *Technique Information Series*: G.E. Research and Development Center, Jan. 2002.

[8] J. D. Choi and W. E. Stark, "Performance of ultra-wideband communications with suboptimal receivers in multipath channels," *IEEE J. Select. Areas Commun.*, vol. 20, no. 9, pp. 1754-1766, Dec. 2002.

[9] Y.-L. Chao and R. A. Scholtz, "Optimal and suboptimal receivers for ultra-wideband transmitted reference systems," *Proc. IEEE Global Telecommunications Conf.*, vol. 2, Dec. 2003, pp. 759-763.

[10] IEEE P802.15-02/368r5-SG3a, "Channel Modeling Sub-committee Report Final," Nov. 18, 2002.

[11] D. M. Pozar, "Waveform optimizations for ultra-wideband radio systems," *IEEE Trans. Antennas and Propagation*, vol. 51, pp. 2335-2345, Sep. 2003.

[12] J. M. Cramer, R. A. Scholtz, and M. Z. Win, "Evaluation of an ultra-wideband propagation channel," *IEEE Trans. Antennas and Propagation*, vol. 50, no. 5, pp. 561-570, May 2002.

[13] K. S. Miller, *Multidimensional Gaussian Distributions*, Wiley, 1964.

[14] M. Abramowitz and I. A. Stegun, *Handbook of Mathematical Functions with Formulas, Graphs, and Mathematical Tables*, New York: Dover Publications, 1970.

[15] I. S. Gradshteyn and I. M. Ryzhik, *Table of Integrals. Series, and Products*, Academic Press, 1980.

[16] Y.-L. Chao and R. A. Scholtz, "Weighted correlation receivers for ultra-wideband transmitted reference systems," *Proc. IEEE Global Telecommunications Conf.*, Vol.1, Dec. 2004, pp. 66-70.

[17] M. K. Simon and M.-S. Alouini, *Digital Communication over Fading Channels: A Unified Approach to Performance Analysis*, John Wiley and Sons, Inc., 2000.

[18] M.-S. Alouini and A. J. Goldsmith, "A unified approach for calculating error rates of linearly modulated signals over generalized fading channels," *IEEE Trans. Commun.*, vol. 47, no. 9, pp. 1324-1334, Sep. 1999.

[19] T. Q.S. Quek and M. Z. Win, "Ultrawide bandwidth transmitted-reference signaling," *Proc. IEEE Int. Conf. Communication*, vol. 6, Jun. 2004, pp. 3409-3413.

[20] Y.-L. Chao, "Optimal integration time analysis for ultra-wideband correlation receivers," *Proc. Asilomar Conf. Signals, Systems and Computers*, Nov. 2004.

[21] G. L. Turin, "The characteristic function of hermitian quadratic forms in complex normal variables," *Biometrika*, vol. 47, No. 1/2, pp. 199-201, June 1960.

[22] M. Pausini, G, Janssen and K. Witrisal, "Analysis of ISI for an IR UWB symbol-differential autocorrelation receiver," *Proc. IEEE Vehic. Technol. Conf.*, Vol. 2, Sep. 2004, pp. 1213-1217.

[23] K. Witrisal and M. Pausini, "Equivalent system model of ISI in a frame-differential IR-UWB receiver," *Proc. IEEE Global Telecommunications Conf.*, Vol. 6, Dec. 2004, pp. 3505-3510.

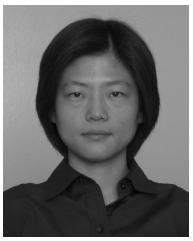

Yi-Ling Chao received the B.S and M.S degrees in electrical engineering from National Central University, Chung-Li, Taiwan, in 1995 and 1997, respectively, and the Ph.D. degree in electrical engineering from the University of Southern California (USC), Los Angeles, in 2005.

From 1997 to 2000, she was with the Industrial Technology Research Institute of Taiwan, where she designed and developed IEEE 802.11b system IC. From 2000 to 2005, she was a Research Assistant with the Ultra-Wideband Radio Laboratory (UltRa Lab), USC. At USC, she primarily worked on UWB radios with transmitted reference methods. Her current research interests include UWB radios, spread spectrum systems, communication theory, and digital signal processing.

Robert A. Scholtz was born in Lebanon, OH, on January 26, 1936. He is a Distinguished Alumnus of the University of Cincinnati, where, as a Sheffield Scholar, he received the Degree in Electrical Engineer in 1958. He was a Hughes Masters and Doctoral Fellow while obtaining his MS and PhD degrees in Electrical Engineering from USC in 1960 and Stanford University in 1964 respectively.

Dr. Scholtz, working on missile radar signal processing problems, remained part-time at Hughes Aircraft Co. until 1978. In 1963, Dr. Scholtz joined the faculty of the University of Southern California, where he is now the Fred H. Cole Professor of Engineering. From 1984 through 1989, he served as Director of USC's Communication Sciences Institute, and from 1994 to 2000 he was Chairman of the Electrical Engineering Systems Department. In 1996 as part of the Integrated Media Systems Center effort, Dr. Scholtz formed the Ultrawideband Radio Laboratory (UltRa Lab) to provide facilities for the design and test of impulse radio systems and other novel high-bandwidth high-data-rate wireless mobile communication links. He has consulted for the LinCom Corp., Axiomatix, Inc., the Jet Propulsion Laboratory, Technology Group, TRW, Pulson Communications (Time Domain Corporation), and Qualcomm, as well as various government agencies.

His research interests include communication theory, synchronization, signal design, coding, adaptive processing, and pseudonoise generation, and their application to communications and radar systems. He has co-authored three books, *Spread Spectrum Communications*, *Spread Spectrum Communications Handbook* with M. K. Simon, J. K. Omura, and B. K. Levitt, and *Basic Concepts in Information Theory and Coding* with S. W. Golomb and R. E. Peile. In 1980, Dr. Scholtz was elected to the grade of Fellow in the IEEE, "for contributions to the theory and design of synchronizable codes for communications and radar systems." He has received many prizes for his research, including the Donald Fink Prize (IEEE), the Leonard G. Abraham Prize Paper Award (IEEE Communications Society), the 1992 Senior Award (IEEE Signal Processing Society), the Ellersick Award (IEEE Military Communications Conference), the Military Communications Conference Award for Technical Achievement, the S. A. Schelkunoff Transactions Prize Paper Award (IEEE Antennas and Propagation Society), and the IWUWBS Best Paper Award (International Workshop on Ultrawideband Systems). In 2004 he delivered the Plenary Address to the joint meeting of IEEE Conference on Ultra Wideband Systems and Technologies and the International Workshop on Ultra Wideband Systems.

Dr. Scholtz has been an active member of the IEEE for many years, manning several organizational posts, including Finance Chairman for the 1977 National Telecommunications Conference, Program Chairman for the 1981 International Symposium on Information Theory, and Board of Governors positions for the Information Theory Group and the Communications Society. He has been General Chairman of six workshops in the area of communications, including most recently two ultrawideband radio workshops held in May 1998 and October 2002 (the latter jointly with Intel).